JACS
JOURNAL OF THE AMERICAN CHEMICAL SOCIETY

Article

pubs.acs.org/JACS

# Computation and Experiment Reveal That the Ring-Rearrangement Metathesis of Himbert Cycloadducts Can Be Subject to Kinetic or Thermodynamic Control

Jonathan K. Lam,[†,§] Hung V. Pham,[‡,§] K. N. Houk,*[,‡] and Christopher D. Vanderwal*[,†]

[†]1102 Natural Sciences II, Department of Chemistry, University of California, Irvine, California 92697-2025, United States

[‡]Department of Chemistry and Biochemistry, University of California, Los Angeles, 607 Charles E. Young Drive, Los Angeles, California 90095-1569, United States

Supporting Information

**ABSTRACT:** Unusual observations in the ring-rearrangement metathesis of Himbert arene/allene cycloadducts to form fused polycyclic lactams led to a more in-depth experimental study that yielded conflicting results. Differences in reactivity within related systems and unexpected changes in diastereoselectivity among other similar substrates were not readily explained on the basis of the experimental results. Computational investigations demonstrated substrate-dependent changes in reaction pathways (ring-opening metathesis/ring-closing metathesis [ROM/RCM] cascade vs ring-closing metathesis/ring-opening metathesis [RCM/ROM] cascade). Furthermore, some reactions were judged to be under thermodynamic control and others under kinetic control. The greater understanding of the most likely reaction pathways and their energetics provides a reasonable explanation for the previously irreconcilable results.

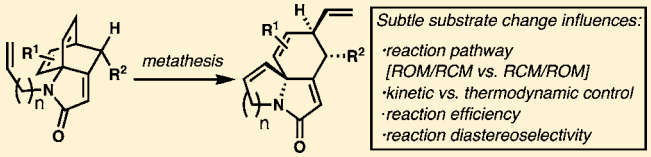


## INTRODUCTION

We recently reported[1] the use of the Himbert arene/allene intramolecular Diels–Alder (IMDA) reaction[2] to generate strained bridged polycyclic lactams that are, in many cases, excellent substrates for ring-rearrangement metathesis to afford the corresponding fused isomeric polycycles (Scheme 1). However, upon delving deeper into this chemistry, we found several substrates that unpredictably did not undergo metathesis rearrangement, some examples of unexpectedly diastereoselective rearrangements, and some interesting qualitative differences in metathesis reaction rates among quite similar substrates. Taken together, these observations suggested some mechanistic subtleties that we felt were worth exploration given the importance of the bridged-to-fused metathesis rearrangement strategy in complex molecule synthesis.[3]

## BACKGROUND

The ring strain in bridged bicycles, especially in bicyclo[2.2.1]heptanes but also in bicyclo[2.2.2]octanes, as well as in their heterocyclic variants, has long been used as a driving force for rearrangement of these ring systems. Frequently, the substrates are made by cycloaddition chemistry. Starting with the synthesis of capnellene by Stille and Grubbs reported in 1986 (Figure 1a),[4] and especially over the past two decades, alkene metathesis has been used extensively to rearrange strained bridged bicyclic structures when a suitable pendant alkene is present;[3] in its absence, many of these strained ring systems act as effective monomers for ring-opening metathesis polymerization (ROMP) (Figure 1b).[5] Likely because of the effectiveness of the ROMP process, it appears that these related ring-rearrangement metathesis processes are often assumed to be initiated via ring-opening metathesis driven by relief of ring strain. However, Grubbs clearly demonstrated in 1996 that strain is not a prerequisite for some types of metathesis cascades when his group showed that even cyclopentenes and cyclohexenes bearing two tethered alkenes can undergo productive rearrangements (Figure 1c);[6] in this case, the entropic benefit of the loss of ethylene drives the rearrangement equilibrium. In that paper, the authors reasoned that initiation likely proceeds at the monosubstituted tethered alkene in preference to the disubstituted ring alkene but that initiation at the ring alkene might well be dominant with sufficient ring strain. Accordingly, both initiation mechanisms might be plausible in many cases, particularly if the ring system is not highly strained. One of the many elegant applications of ring-rearrangement metathesis to complex molecule synthesis can be seen in Figure 1d, wherein the Phillips group rearranged oxanorbornene **14** to fused bicyclic product **15**;[7] the site of initiation of this key transformation en route to kumausyne has apparently not been determined. Finally, and surprisingly, Fallis has recently shown using careful NMR and deuterium-labeling studies that the ring-rearrangement metathesis of alkene-tethered norbornenes is not initiated by ring-opening metathesis but rather by metathesis of the pendant alkene (Figure 1e).[8] In all of the examples in Figure 1 other than the cyclopentene ring rearrangement (Figure 1c), it would appear plausible that there is sufficient ring strain in the starting

**Received:** September 16, 2013
**Published:** October 10, 2013

 © 2013 American Chemical Society  dx.doi.org/10.1021/ja409618p | J. Am. Chem. Soc. 2013, 135, 17585–17594

**Scheme 1. Sequential Use of the Himbert Arene/Allene Intramolecular Diels–Alder (IMDA) Reaction and Ring-Rearrangement Metathesis To Afford Fused Polycyclic Lactams**

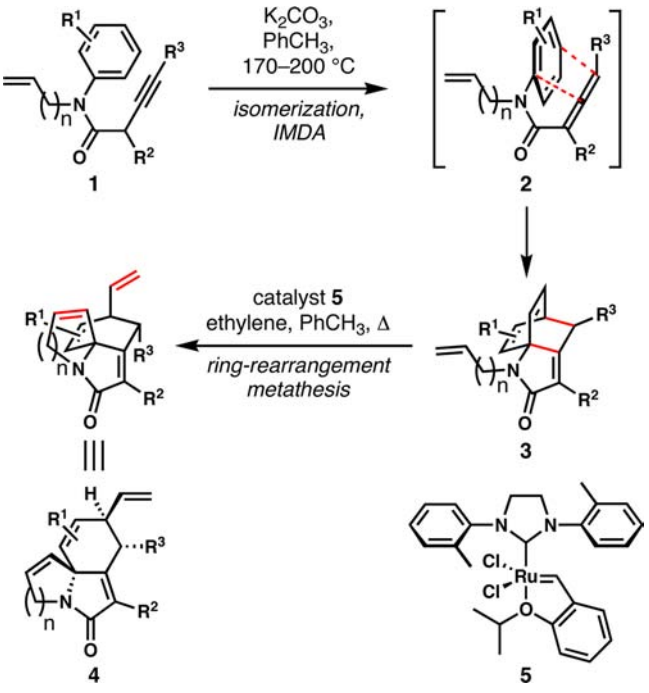


materials to render these reactions essentially irreversible and therefore kinetically controlled, although no distribution of related products would be expected in any of these contexts.

In the context of our work on the rearrangement of Himbert cycloadducts, we have found what we believe to be a substrate-dependent change in mechanism for these rearrangement reactions, which we describe in detail in this report. Moreover, some unusual stereochemical results can be rationalized on the basis of this mechanistic dichotomy. Some of these unusual findings might be explained by a deviation from the expected kinetic control in strain-driven ring-rearrangement metathesis; experimental and computational results both suggest that many of the rearrangements of Himbert cycloadducts are under thermodynamic control.

## RESULTS AND DISCUSSION

**Ring-Rearrangement Metathesis: Order of Steps.** Our first general foray into the ring-rearrangement metathesis of Himbert cycloadducts dealt with achiral tricyclic lactams bearing pendant alkenes on nitrogen (Figure 2). Substrate

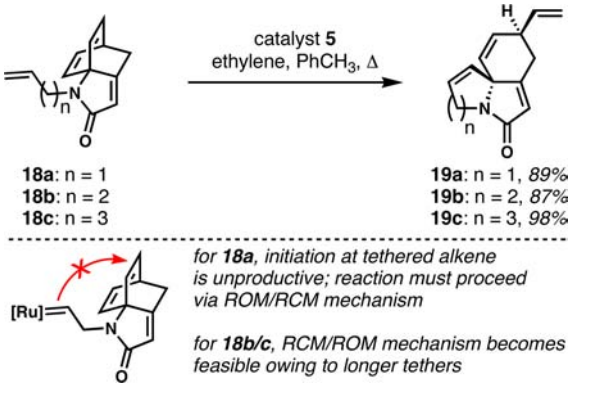


**Figure 2.** Ring-rearrangement metathesis of achiral tricyclic lactams **18a–c**.

**18a** underwent rearrangement smoothly under catalysis by second-generation Hoveyda–Grubbs-type catalyst **5**,[9] although heating in toluene (minimum 50 °C, usually carried out at 100 °C) under an atmosphere of ethylene was required. With this substrate, initiation by metathesis with the pendant alkene is

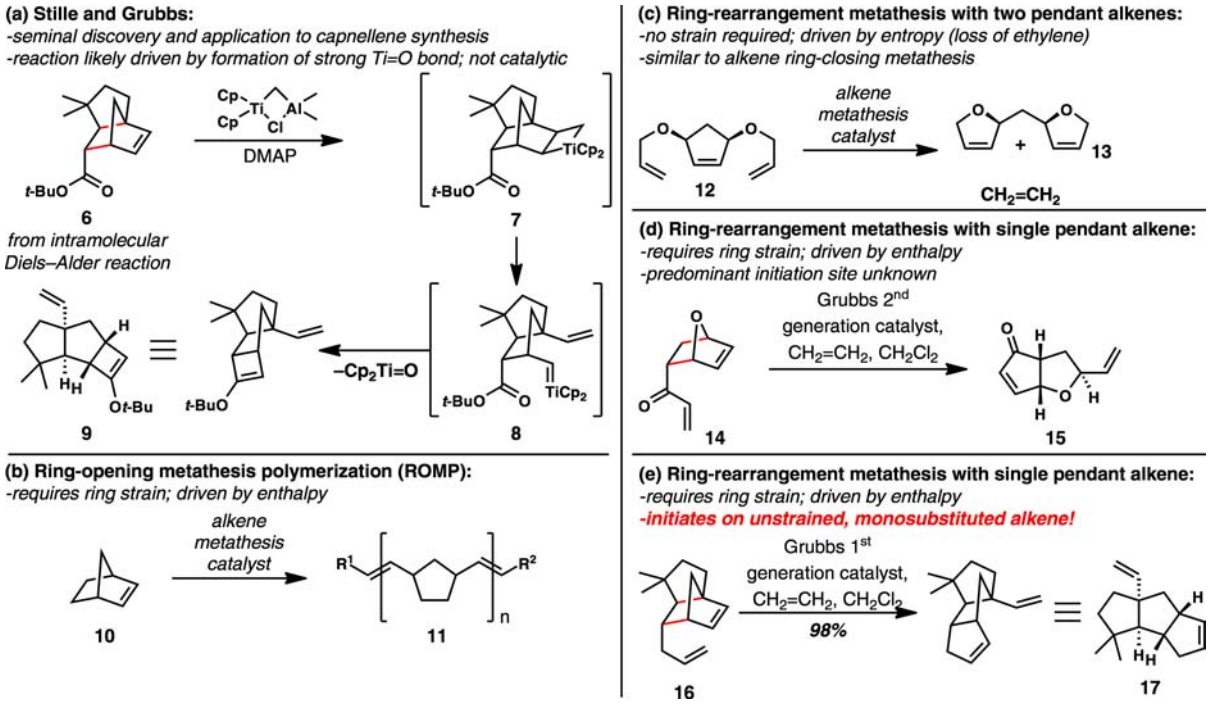


**Figure 1.** Important relevant examples of ring-rearrangement metathesis and the related ring-opening metathesis polymerization (ROMP) process.


dx.doi.org/10.1021/ja409618p | J. Am. Chem. Soc. 2013, 135, 17585–17594

not feasible because geometric constraints preclude the intermediate ruthenium alkylidene from reacting with the strained alkene of the bicyclo[2.2.2]octadiene system; therefore, productive rearrangement must be initiated with ring-opening metathesis. Systems **18b** and **18c**, with homologous tethered alkenes, reacted under the same conditions to give the rearranged products in high yield, but these reactions were significantly faster than the one with allylic amine **18a**. This observation suggested that initiation occurred at the unstrained pendant alkene (RCM/ROM pathway) for **18b** and **18c**, because if ROM were the initiating step, then the subsequent RCM steps might be expected to be slower with increasing ring size, not faster, if the ring closure were the rate-determining step. That supposition assumes that the ROM process would transpire at similar rates regardless of the nature of the tethered alkene. These rather trivial observations and the logical conclusions that followed piqued our interest in the mechanistic subtleties of these reactions.

Much more dramatic results were generated with the closely related chiral (racemic) tricyclic lactams that were obtained via Himbert cycloaddition of $\gamma$-methyl-substituted allene (Figure 3). These cycloadducts (**20a–c**) reacted productively under

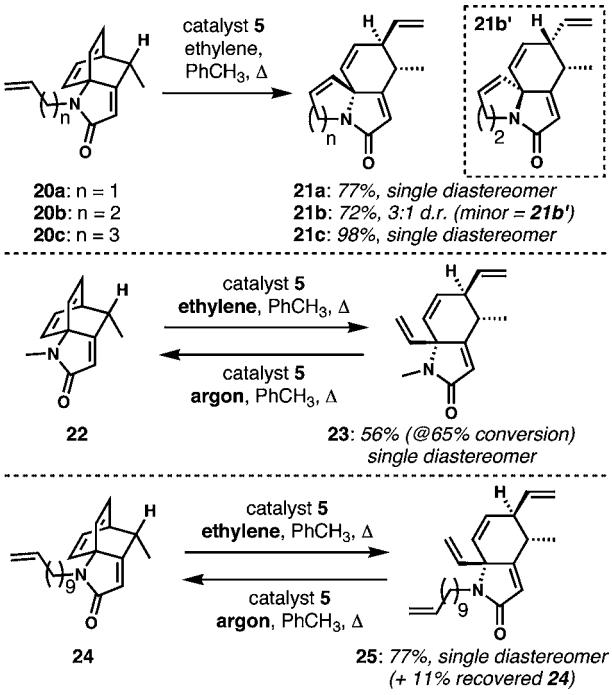


**Figure 3.** Unusual stereochemical results in the ring-rearrangement metathesis reactions of chiral tricyclic lactams (starting materials and products were racemic).

our standard conditions to afford the fused products **21a–c**; however, there was a surprising difference in the stereochemical outcomes. Whereas the *N*-allyl and *N*-pentenyl substrates rearranged to afford single isomers of the product to the limits of detection by $^1$H NMR spectroscopy, the *N*-butenyl substrate **20b** delivered a 3:1 ratio of diastereomers. As a further data point, the *N*-methyl congener **22** was subjected to the same conditions, and the ring-opened ethenolysis product **23** was obtained as a single diastereomer. When **23** was exposed to metathesis catalyst **5** *without ethylene*, bridged tricyclic compound **22** was regenerated (80% yield, 10% recovered **23**). We also attempted ring-rearrangement metathesis of the *N*-undecenyl substrate **24**, and only ring-opened product **25** was obtained. In an attempt to form the 13-membered ring, **25** was exposed to catalyst **5** in dilute solution (no ethylene); tricyclic product **24** was formed in 73% yield. These two examples clearly demonstrate that there is sufficiently little strain in the tricyclic cycloadducts that ring closure can be effected when coupled to the entropically favored release of ethylene.

In the series **20a–c**, only the reaction of **20a** absolutely required ethylene; **20b** and **20c** did not (this dichotomy was also observed with **18a** and **18b**, but **18c** was not tested). These results are consistent with preferential reactivity of the pendant alkene over the cyclic alkene; for *N*-allyl substrates **18a** and **20a**, RCM is not feasible because of the short tether (see Figure 2) and ethylene presumably allows for rapid disengagement of the catalyst. For the longer tethers, of course, RCM should be possible and ethylene should play a lesser role in the reaction outcome.

Initially, we expected that these metathesis processes would afford a kinetic distribution of products that should be governed by which diastereotopic ring alkene reacted preferentially. Further, we assumed that catalyst approach would be preferred "between" the two alkenes, which did not offer obvious possibilities for high levels of diastereocontrol. Therefore, we were surprised to observe high diastereoselectivity in many cases and were even more intrigued by the difference with substrate **20b**. We considered that there might be an unexpected preference for catalyst approach from the other side of the reactive alkenes, which would permit the methyl group on the stereogenic carbon to play a role in determining the regioselectivity of metathesis initiation, ultimately dictating the stereochemical outcome of the reaction. While that idea might reasonably account for the outcome of the reaction of **20a**, in which initiation of the rearrangement must occur at the ring alkenes, it does not explain in a clear way why the selectivity decreases with **20b** while the reaction of **20c** is again exquisitely selective.

A third striking set of data was obtained from the attempted ring-rearrangement metathesis of the homologous series of benzo-fused cycloadducts shown in Figure 4. In this particular series, only *N*-butenyl substrate **26b** reacted to afford fused tetracyclic product **27b**; substrates with other tether lengths were recovered unchanged, without ethenolysis of the bicyclic

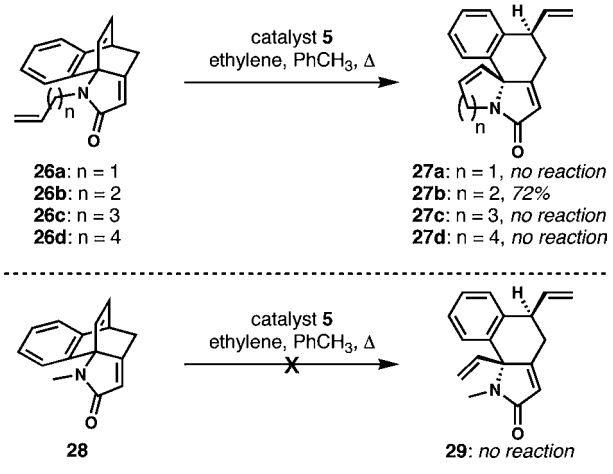


**Figure 4.** Unusual ring-rearrangement metathesis results with benzo-fused substrates.


dx.doi.org/10.1021/ja409618p | J. Am. Chem. Soc. 2013, 135, 17585–17594

system. As a control experiment, *N*-methyl substrate **28** was subjected to metathesis conditions, and it too was recovered unchanged. The differences in the reactivities of these benzo-fused systems and the simpler tricycles shown in Figure 2 were unanticipated. Certainly, a steric impediment to productive ring closure was suspected, but it was not obvious why **26b** would react successfully while the other substrates were unreactive.

Finally, the cycloadducts ultimately derived from 2,3-dimethylaniline (Figure 5) led to further confusion, as

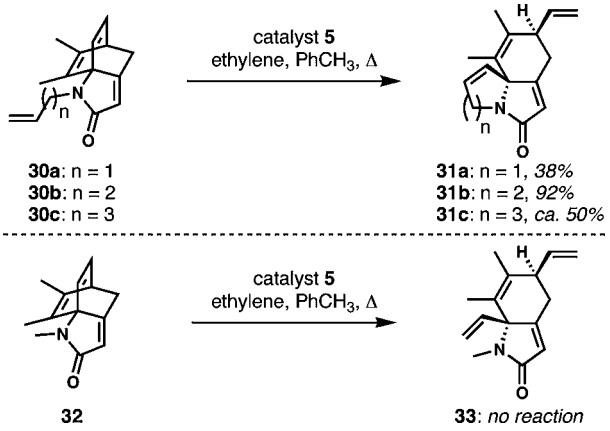


**Figure 5.** Metathesis experiments on cycloadducts derived from 2,3-dimethylaniline.

(moderately) successful rearrangements were observed in all cases examined, but the ring-opening ethenolysis of **32** failed. We were at a loss to explain differences in the reactivities of the series **26a–c** and **30a–c** given what must be similar steric environments about the relevant alkenes.

**Computation Clarifies the Unusual Experimental Results.** *General Computational Study Design.* As a whole, the results shown in Figures 2 through 5 could not be easily reconciled, and it was not clear that further experiments would aid in the development of a working model to understand this family of rearrangement reactions. When faced with situations in which the collection of more experimental data is not likely to increase our understanding of the reaction mechanisms or outcomes, our UCI and UCLA groups have engaged in fruitful collaborations, with the latter group providing expertise in DFT calculations of ground-state energies and transition states.[1b,10] In this section, we will demonstrate how the collection of aberrant/unexpected results described above can in fact be reconciled via careful consideration of both kinetic and thermodynamic reaction parameters; the key data required to shed light on the unusual experimental outcomes could be obtained only by calculation.

The mechanisms of ring-opening and ring-closing metatheses have been studied extensively by computation in recent decades,[11] but ring-rearrangement metathesis has received less focus.[3a,12] We began our investigation by determining the chemoselectivity of initiation of the ring-rearrangement meta-

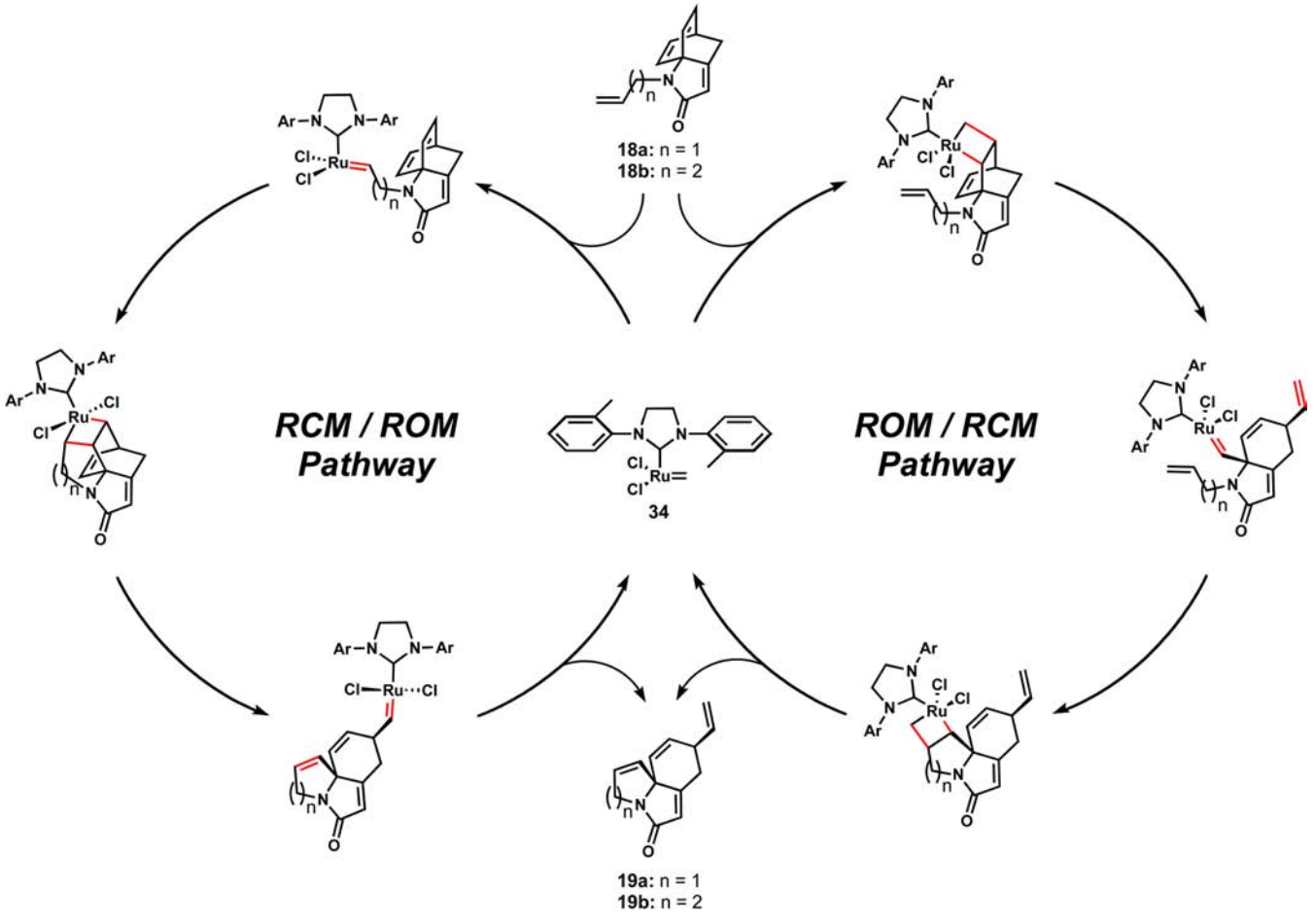


**Figure 6.** Two possible orders of events for the ring-rearrangement metatheses of representative Himbert cycloadducts **18a** and **18b**.


dx.doi.org/10.1021/ja409618p | J. Am. Chem. Soc. 2013, 135, 17585–17594

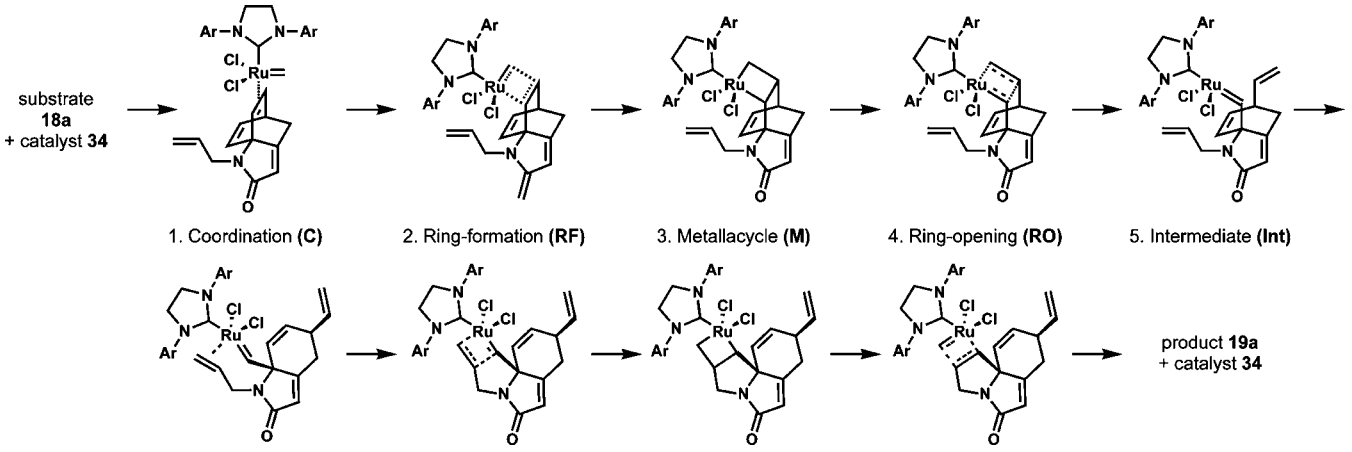


**Figure 7.** The five different types of stationary points considered in the computational results described herein, as exemplified in the ROM/RCM mechanism for **18a**. It should be noted that within each cascade, the first four types stationary points recur in each cycle.

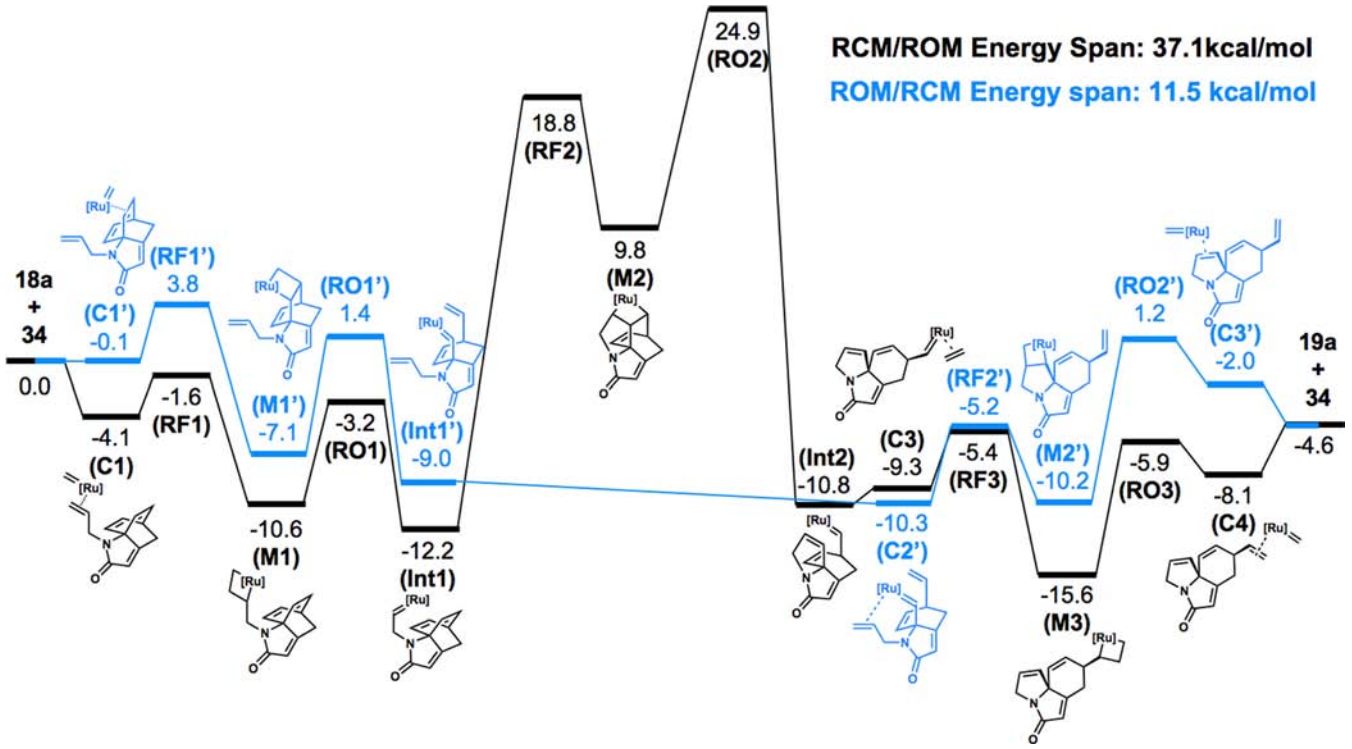


**Figure 8.** Computational comparison of the RCM/ROM and ROM/RCM pathways for the metathesis rearrangement of **18a** suggests a strong preference for the ROM/RCM pathway via an equilibrating process. M06/6-311+G(d,p)/SDD//B3LYP/6-31G(d)/LANL2DZ, SMD:Toluene.

thesis of substrates **18a** and **18b**, which differ by only one carbon in the tether, to determine whether the tether length influences which process (ROM or RCM) occurs first. The two pathways are shown in Figure 6, with key intermediates shown along each route. In the ROM/RCM manifold, the (somewhat) strained cyclic alkene of the bridged tricyclic system is engaged first, leading to ring opening. An important consideration here involves the regiochemistry of the reaction: two different ruthenium alkylidenes can be formed, and only one is able to proceed to product by ring closure onto the tethered alkene. The other regioisomer (not shown) would require ring closure back to the starting tricyclic system followed by opening to afford the only productive regioisomer. In the RCM/ROM pathway, the terminal alkene is engaged first, and the cyclic alkene can react only with the tethered ruthenium alkylidene in one regioisomeric sense because of geometrical constraints.

Prior investigations of metathesis cascades have established a Chauvin-type mechanism[13] that generally consists of five relevant stationary points (Figure 7, shown for the ROM/RCM reaction of **18a**): (1) coordination of the catalyst to the substrate, (2) a transition state for the formation of the metallacycle, (3) a metallacycle intermediate, (4) a transition state for the metallacycle ring opening, and (5) the newly formed alkylidene intermediate or product. For both the ROM/RCM and RCM/ROM cascades, there are multiple distinct stationary points of types (1) through (4), as shown in the figure for the ROM/RCM manifold.

All of the structures shown in Figure 7 were optimized using the B3LYP density functional with a LANL2DZ basis set for


dx.doi.org/10.1021/ja409618p | J. Am. Chem. Soc. 2013, 135, 17585−17594

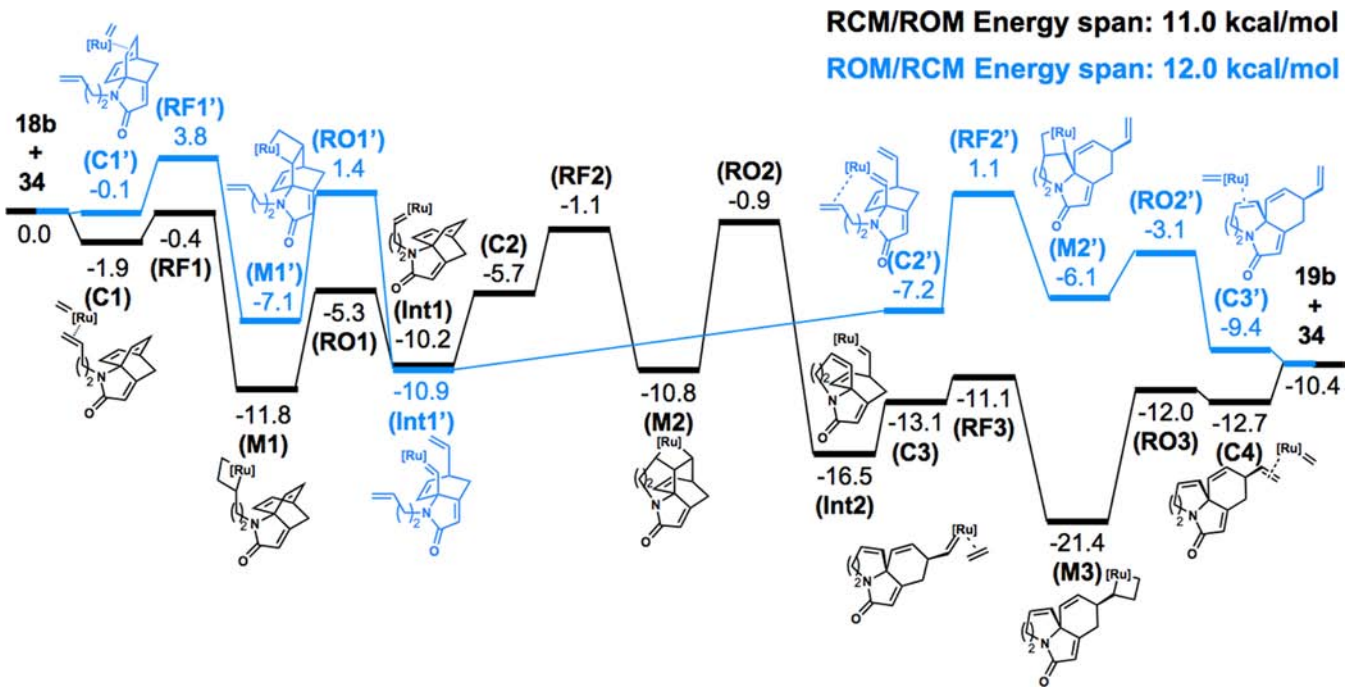


**Figure 9.** Computational comparison of the RCM/ROM and ROM/RCM pathways for the metathesis rearrangement of **18b** suggests a preference for the RCM/ROM pathway via a kinetically controlled process. M06/6-311+G(d,p)/SDD//B3LYP/6-31G(d)/LANL2DZ, SMD:Toluene.

the ruthenium atom of the catalyst and a 6-31G(d) basis set for the carbon, oxygen, nitrogen, and hydrogen atoms.[14] Single-point energies were calculated with the M06 functional using the mixed basis set of SDD for Ru and a 6-311+G(d,p) basis set for the remaining atoms.[11n,15] This protocol has been successfully applied in prior metathesis investigations.[16] The SMD model for toluene was used for solvation energy corrections.[17]

Although the precatalyst **5** consists of a benzylidene ligand and a chelating isopropoxy group, initiation under an ethylene atmosphere generates the active species **34** that participates in the catalytic cycle. Initiation of **5** has been studied extensively before, and thus, we used **34** as our model catalyst in all of the calculations.[18]

*Mechanistic Differences among Substrates **18a–c**.* The free energy profiles for the ROM/RCM and RCM/ROM cascades of *N*-allyl substrate **18a** are shown in Figure 8. Catalyst **34** (derived from precatalyst **5**) initially prefers to react with the pendant alkene, forming **Int1** of the RCM/ROM pathway. However, the short *N*-allyl tether cannot allow the formation of **M2** without introducing significant strain into the polycyclic system. This restriction results in transition state **RO2** having an insurmountable free energy 37.1 kcal/mol higher than that of **Int1**, ultimately ruling out the RCM/ROM pathway for **18a**. Conversely, initial ring opening of the bicyclo[2.2.2]octadiene leads to a more reasonable energy span[19] of 11.5 kcal/mol, calculated as the energy difference between the lowest-lying intermediate (**C2′**) and the highest subsequent barrier (**RO2′**). Because the reaction is favored by only about 5 kcal/mol and also because of the relatively small energy barriers involved, this reaction should be fully reversible (under thermodynamic control).[20] Depending on the approach of the ruthenium catalyst, various ring-opening pathways are reasonable. We computationally studied each reasonable pathway, but the one shown here in which ROM and RCM occur intramolecularly (without dissociation/association of the catalyst with the help of a molecule of ethylene) is the most plausible, containing the lowest energy span. Hence, **18a** follows an ROM/RCM mechanism because of its shorter tether length, a result that one could rationalize without computation in this case but that nonetheless provides an excellent starting point for this study.

The *N*-butenyl-substituted substrate **18b** exhibits substantially lower strain in the ring-closing and ring-opening steps associated with metallacycle **M2** of the RCM/ROM pathway (Figure 9). The longer tether allows the adoption of a favorable conformation for the intramolecular metathesis reaction to occur, thereby lowering the energy span for the RCM/ROM pathway to 11 kcal/mol. The ROM/RCM cascade, in contrast, is relatively unaffected by the longer tether of **18b**, resulting in a free energy profile similar to that for **18a**. We should note that the initial steps of this pathway (**C1′** to **RO1′**) were not explicitly calculated for **18b**; rather, these energies were taken from **18a** because the tether elongation from **18a** to **18b** is remote from the reaction site and should not appreciably affect the energetics of these stationary points. Although the RCM/ROM and ROM/RCM energy spans are comparable—an energy span of 11.0 kcal/mol for RCM/ROM is determined as the energy difference between low-lying intermediate **M3** and extruded product **19b**, while the ROM/RCM energy span is 12.0 kcal/mol from alkylidene **Int1′** to metallocyclobutene transition state **RF2′**—the preference for catalyst attack at the less hindered alkene tether points toward RCM/ROM as the dominant pathway. Moreover, the low-lying intermediate **M3** prevents the backward trajectory from occurring, since it would require greater than 20 kcal/mol (back to **RF2**) compared to the 11 kcal/mol needed for the extrusion of product. This large preference for the forward reaction, which is not present in the ROM/RCM cascade for **18a**, also very nicely explains the observed disparity in diastereoselectivity between chiral substrates **20a** and **20b** (see below).

*Consequences in the Stereoselectivity of Rearrangement of Chiral Substrates **20a–c**.* Our computational studies


dx.doi.org/10.1021/ja409618p | J. Am. Chem. Soc. 2013, 135, 17585–17594

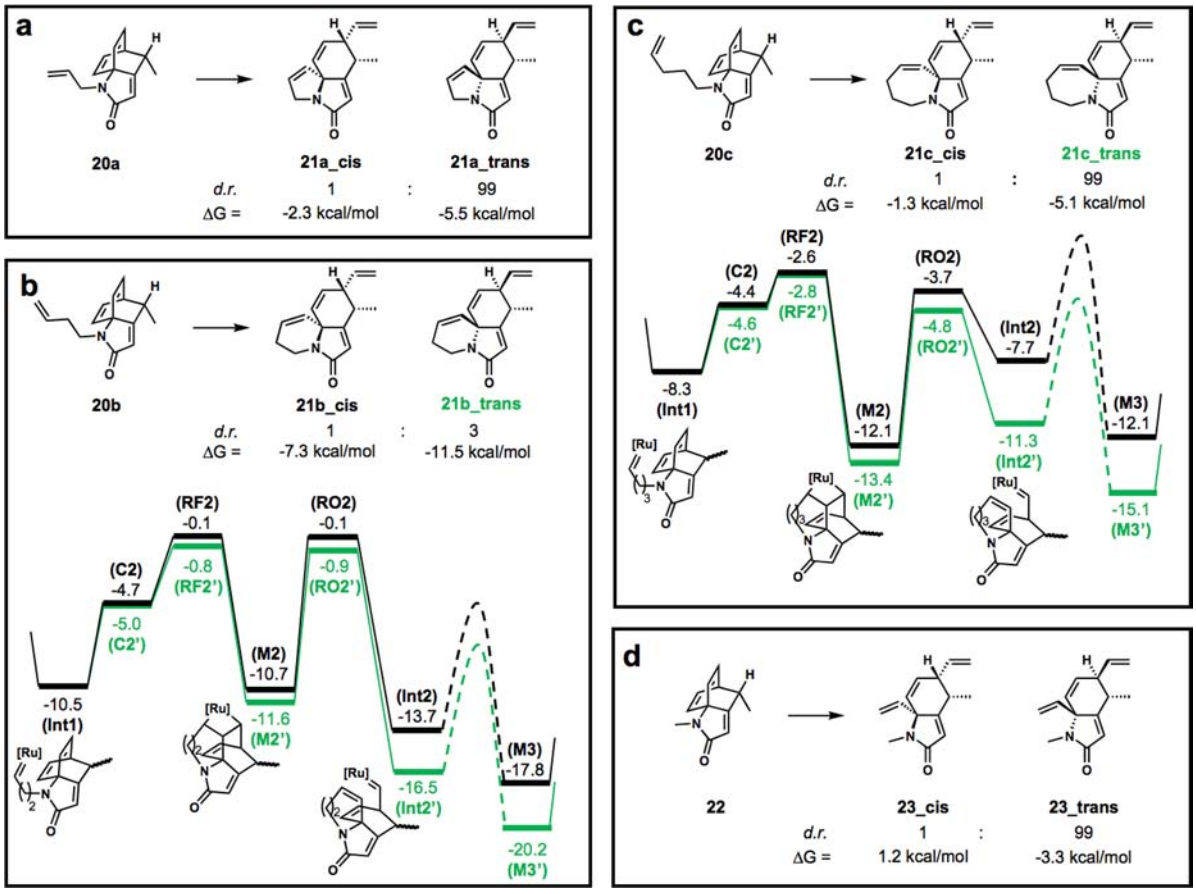


**Figure 10.** Consideration of the diastereoselectivity of ring-rearrangement metathesis of chiral, methyl-substituted Himbert cycloadducts **20a–c** and **22**. (a) The rearrangement of **20a** (ROM/RCM) is thermodynamically controlled, and only **21a_trans** is observed. (b) The rearrangement of **20b** (RCM/ROM) is kinetically controlled, and a 3:1 ratio of products **21b_trans** and **21b_cis** is observed. (c) The rearrangement of **20c** (RCM/ROM) is thermodynamically controlled, and only **21a_trans** is observed. (d) The ring-opening ethenolysis of **22** is thermodynamically controlled, and only **23_trans** is observed. M06/6-311+G(d,p)/SDD//B3LYP/6-31G(d)/LANL2DZ, SMD:Toluene. *d.r.* values are from experiment, and free energies (Δ*G*, in kcal/mol) are from DFT calculations.

indicate that the favored ROM/RCM pathway for **18a**, and analogously for the methylated **20a**, does not have a strong preference to proceed to product from low-lying intermediate **C2′**, as there is only a 2.6 kcal/mol difference between **RO2′** and **RF1′**, the rate-determining steps of the forward and backward reactions, respectively. Consequently, the chiral substrate **20a** should equilibrate between intermediates until product formation and release, and the ratio of diastereomeric products is governed by the reaction thermodynamics. The calculated free energies (DFT) show that **21a_trans** is favored over **21a_cis** by 3.2 kcal/mol, consistent with the experimental observation of only the trans isomer (Figure 10a).

On the other hand, since the reaction profile of **20b** should closely resemble that of **18b**, where the formation of **Int2** exclusively leads to product and equilibration with prior intermediates is not viable, the stereoselectivity is determined by the RCM steps **Int1** to **Int2**. Thus, the ratio of **21b_trans** and **21b_cis** is controlled by the energy difference between rate-determining barriers **RO2** and **RF2′** and not the calculated product energies shown. The computations predict a 0.7 kcal/mol preference for the major product **21b_trans**, which translates to ca. 3:1 dr at 100 °C (Figure 10b).

Metathesis of the longer pentenyl-substituted **20c** resulted in the formation of **21c_trans** exclusively, which was unexpected since **20c** contains a sufficiently long tether to proceed through the RCM/ROM pathway (similar to **20b**) but **RF2** and **RF2′** are virtually degenerate (Figure 10c). The higher energy of **M3** accounts for this peculiarity; the large propensity for **Int2** to proceed in the forward direction is now diminished because of the facility of reversion back to **Int1**. The 5.1 kcal/mol required to recross **RF2** is now comparable to the ∼5 kcal/mol needed to overcome **RF3** to achieve metallocyclobutane **M3**. Moreover, product **21c_cis** is higher in energy than **RF2**, suggesting that the backward reaction to form **Int1** is kinetically favored and that eventually only **M3′**, and ultimately **21c_trans**, will be formed. It should be noted that the instability of **Int2** and **Int2′** arise from the strain of the newly formed seven-membered ring, as evidenced by the 6 kcal/mol rise in energy on going from **21b** to **21c** for both isomers.

*N*-Methyl substrate **22** undergoes clean ethenolysis under standard conditions, affording only the trans product (Figures 3 and 10d), and *N*-undecenyl substrate **24** behaves virtually identically (Figure 3). The reaction of **22** is thermodynamically controlled, and the 4.5 kcal/mol preference calculated for the trans isomer is completely consistent with the observed results. While calculations were not performed on the reaction of **24** to afford ethenolysis product **25**, it is reasonable to expect the same behavior as for **22**, with the kinetics of ring closure to a 13-membered ring accounting for the lack of tricyclic products observed. Furthermore, under reaction conditions that exclude


dx.doi.org/10.1021/ja409618p | *J. Am. Chem. Soc.* 2013, 135, 17585–17594

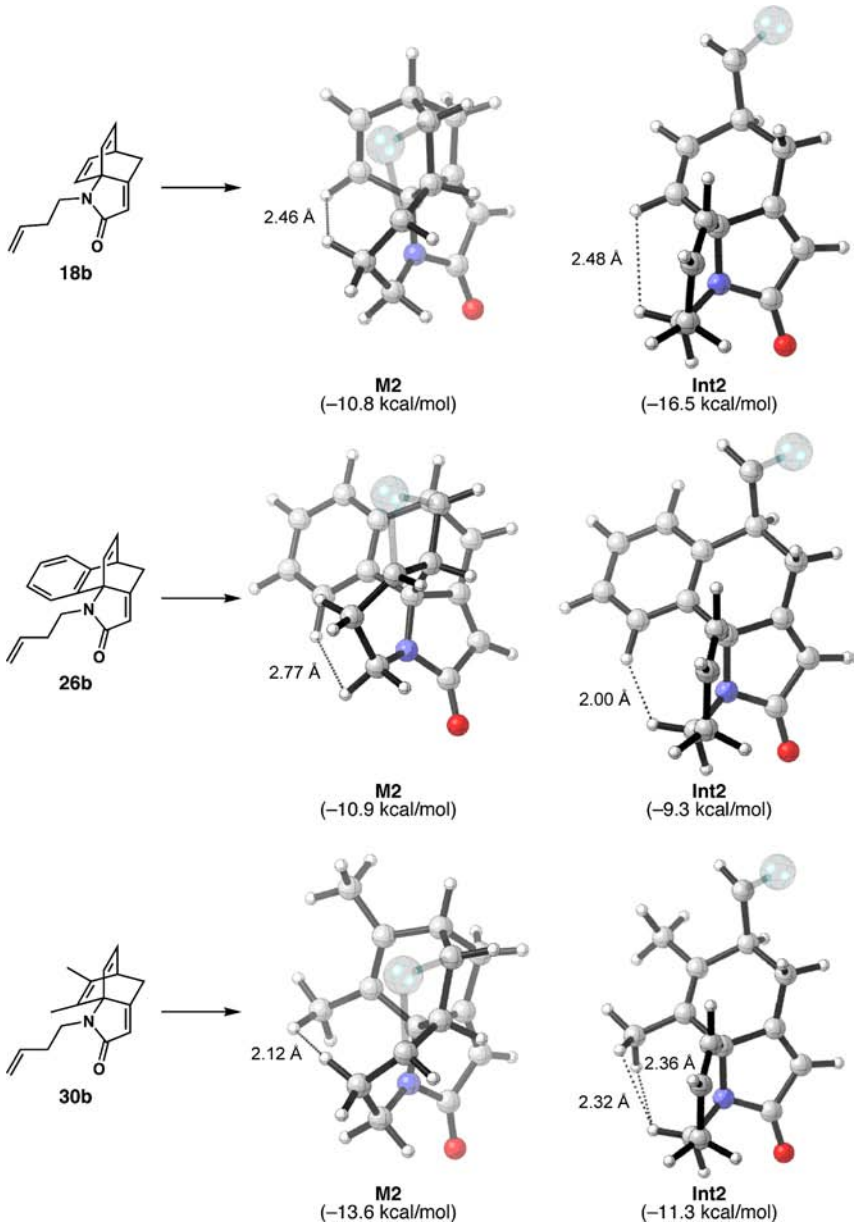


**Figure 11.** Steric strain in intermediates **Int2** for substrates of types **26** and **30** bearing ring alkene substituents raises the energy of those intermediates and results in a thermodynamically controlled reaction. The catalyst architecture has been hidden for clarity. See the Supporting Information for more details.

ethylene, the reverse transformation proceeds to complete conversion.

*An Explanation for the Unusual Results with Benzo-Fused and Ring-Alkene-Substituted Substrates.* A similar explanation can be invoked to explain the reactivity of benzo-fused substrates **26a–d** and alkene-substituted reactants **30a–c**. In addition to **26a** and **30a**, which participate in the "quasi-reversible" ROM/RCM mechanism because of their short tethers, the destabilization of **Int2** provides easier access to the backward reaction for substrates **26b–d** and **30b–c** that undergo RCM/ROM, thereby causing thermodynamics to control the reaction outcomes. Figure 11 illustrates the steric strain that arises in **Int2** after ring-closing metathesis generates the fused carbocycle. Ring alkene substituents that are in proximity of the nitrogen tether destabilize the fused ring system, and this effect also presents itself in the reaction free energies of the products. Hence, by examining the DFT-calculated free energies of reaction in Figure 12, we can predict whether the reaction will be successful, and a clearer picture can be drawn. Metatheses that result in higher-energy products will of course favor the backward reaction, preventing the ring-rearrangement cascade from being productive. The only outlier is the reaction with **26a**, which is predicted to be exergonic but results in no appreciable yield of **27a**. While we do not completely understand that outcome, we do note that the reaction of **26a** requires traversal of one relatively high barrier (compared with the analogous reaction of **18a**, on account of the increased steric strain), which might account for the lack of production of tetracyclic product **27a**.[21]

## ■ CONCLUSIONS

Unusual experimental observations in the course of the bridged-to-fused ring-rearrangement metathesis of Himbert cycloadducts were not readily explained by further experiments.


dx.doi.org/10.1021/ja409618p | J. Am. Chem. Soc. 2013, 135, 17585–17594

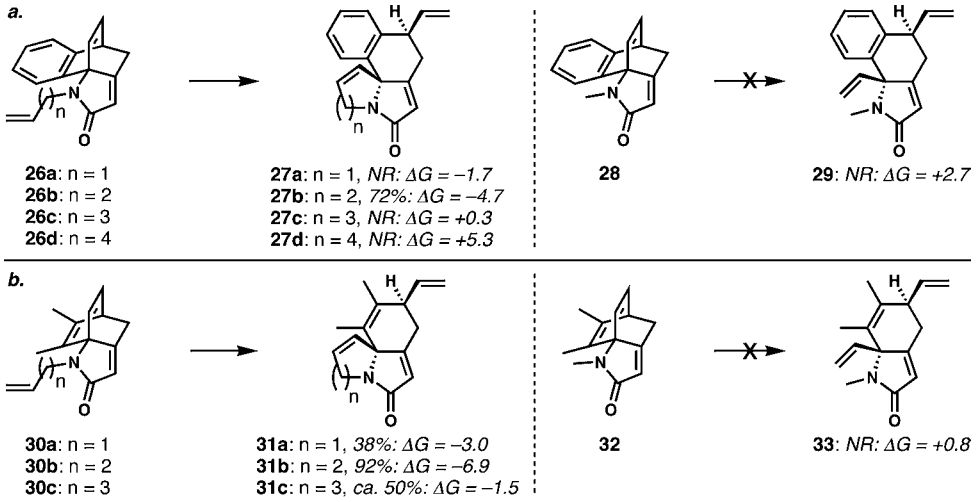


**Figure 12.** The reactions of ring-alkene-substituted systems are under thermodynamic control and can therefore be explained by the free energies of the reactions. (a) Benzo-fused examples **26a−d** and **28**. (b) Ring-alkene-substituted examples **30a−c** and **32**.

Computational interrogation of these data led to reasonable explanations for the previously irreconcilable results. We now understand that in these systems:

1. Initiation of metathesis by the ruthenium catalysts is favored at the monosubstituted, tethered alkene over the bicyclic alkene, despite the potential for relief of ring strain in the latter. As a result, the RCM/ROM pathway is generally favored.

2. If the tether is not sufficiently long to enable an RCM/ROM cascade, then the only productive pathway available is the ROM/RCM cascade, which requires equilibration to ring-opened intermediates.

3. Generally, in the RCM/ROM pathways, the reactions are kinetically controlled because of the irreversibility of the RCM step; however, in the ROM/RCM cascades, the product distribution is thermodynamically controlled because of facile equilibration.

4. In certain substituted cases, sufficient strain can be induced in key metallocyclobutane and ruthenium alkylidene intermediates to raise the energies of these species in such a way as to facilitate equilibration in RCM/ROM systems; in these cases, the reaction free energies can explain the success or failure of the metathesis rearrangements.

These general observations provide satisfactory explanations of the experimentally observed changes in reactivity and diastereoselectivity among closely related substrate groups. The message that transcends the current study is that these and related ring-rearrangement metathesis reactions might often be subject to thermodynamic and not kinetic control. Naturally, this situation is most likely when the reactants are not highly strained, as in the case of the bridged bicyclo[2.2.2]octadiene substructures in this study.[22] Finally, this work serves to reinforce the fact that initiation of ring-rearrangement metathesis cascades is often preferred at a tethered, less substituted alkene[8] rather than the strained and "ostensibly more reactive" ring alkene.

## ■ ASSOCIATED CONTENT

### Supporting Information

Experimental protocols; characterization data; NMR spectra for new compounds; and computational data, including Cartesian coordinates and energies. This material is available free of charge via the Internet at http://pubs.acs.org.

## ■ AUTHOR INFORMATION


### Corresponding Authors

houk@chem.ucla.edu
cdv@uci.edu

### Author Contributions

[§]J.K.L. and H.V.P. contributed equally.


### Notes

The authors declare no competing financial interest.

## ■ ACKNOWLEDGMENTS

We thank the NSERC of Canada and Allergan for graduate fellowships to J.K.L. Work at UC Irvine was supported by the NSF (Awards CHE-0847061 [CAREER] and CHE-1262040). We thank Materia for a generous donation of metathesis catalysts. K.N.H. thanks the National Institute of General Medical Sciences, National Institutes of Health (GM-36770). H.V.P. was funded by the UCLA Graduate Division and is a recipient of the NIH Chemistry−Biology Interface Research Training Grant (USPHS National Research Service Award GM-008469). This work used the Extreme Science and Engineering Discovery Environment (XSEDE), which is supported by the National Science Foundation (Grant OCI-1053575).

## ■ REFERENCES

(1) (a) Lam, J. K.; Schmidt, Y.; Vanderwal, C. D. *Org. Lett.* **2012**, *14*, 5566−5569. (b) Schmidt, Y.; Lam, J. K.; Pham, H. V.; Houk, K. N.; Vanderwal, C. D. *J. Am. Chem. Soc.* **2013**, *135*, 7339−7348.
(2) Himbert, G.; Henn, L. *Angew. Chem., Int. Ed. Engl.* **1982**, *21*, 620.
(3) For reviews, see: (a) Holub, N.; Blechert, S. *Chem.—Asian J.* **2007**, *2*, 1064−1082. (b) Arjona, O.; Csáky, A. G.; Plumet, J. *Eur. J. Org. Chem.* **2003**, 611−622.
(4) Stille, J. R.; Grubbs, R. H. *J. Am. Chem. Soc.* **1986**, *108*, 855−856.
(5) Bielawski, C. W.; Grubbs, R. H. *Prog. Polym. Sci.* **2007**, *32*, 1−29.
(6) Zuercher, W. J.; Hashimoto, M.; Grubbs, R. H. *J. Am. Chem. Soc.* **1996**, *118*, 6634−6640.
(7) Chandler, C. L.; Phillips, A. J. *Org. Lett.* **2005**, *7*, 3493−3495.
(8) Nguyen, N. N. M.; Leclère, M.; Stogaitis, N.; Fallis, A. G. *Org. Lett.* **2010**, *12*, 1684−1687.

(9) (a) Garber, S. B.; Kingsbury, J. S.; Gray, B. L.; Hoveyda, A. H. *J. Am. Chem. Soc.* **2000**, *122*, 8168−8179. (b) Gessler, S.; Randl, S.; Blechert, S. *Tetrahedron Lett.* **2000**, *41*, 9973−9976. (c) Stewart, I. C.; Ung, T.; Pletnev, A. A.; Berlin, J. M.; Grubbs, R. H.; Schrodi, Y. *Org. Lett.* **2007**, *9*, 1589−1592.
(10) (a) Pham, H. V.; Martin, D. B. C.; Vanderwal, C. D.; Houk, K. N. *Chem. Sci.* **2012**, *3*, 1650−1655. (b) Paton, R. S.; Steinhardt, S. E.; Vanderwal, C. D.; Houk, K. N. *J. Am. Chem. Soc.* **2011**, *133*, 3895−3905.
(11) (a) Aagaard, O. M.; Meier, R. J.; Buda, F. *J. Am. Chem. Soc.* **1998**, *120*, 7174−7182. (b) Adlhart, C.; Hinderling, C.; Baumann, H.; Chen, P. *J. Am. Chem. Soc.* **2000**, *122*, 8204−8214. (c) Adlhart, C.; Chen, P. *J. Am. Chem. Soc.* **2004**, *126*, 3496−3510. (d) Torker, S.; Merki, D.; Chen, P. *J. Am. Chem. Soc.* **2008**, *130*, 4808−4814. (e) Bernardi, F.; Bottoni, A.; Miscione, G. P. *Organometallics* **2003**, *22*, 940−947. (f) Cavallo, L. *J. Am. Chem. Soc.* **2002**, *124*, 8965−8973. (g) Cavallo, L.; Correa, A. *J. Am. Chem. Soc.* **2006**, *128*, 13352−13353. (h) Vyboishchikov, S. F.; Bühl, M.; Thiel, W. *Chem.—Eur. J.* **2002**, *8*, 3962−3975. (i) Fomine, S.; Martinez Vargas, S.; Tlenkopatchev, M. A. *Organometallics* **2003**, *22*, 93−99. (j) Suresh, C. H.; Koga, N. *Organometallics* **2004**, *23*, 76−80. (k) Tsipis, A. C.; Orpen, A. G.; Harvey, J. N. *Dalton Trans.* **2005**, 2849−2858. (l) Straub, B. F. *Adv. Synth. Catal.* **2007**, *349*, 204−214. (m) Occhipinti, G.; Bjørsvik, H. R.; Jensen, V. R. *J. Am. Chem. Soc.* **2006**, *128*, 6952−6964. (n) Zhao, Y.; Truhlar, D. G. *Org. Lett.* **2007**, *9*, 1967−1970. (o) du Toit, J. I.; van Sittert, C. G. C. E.; Vosloo, H. C. M. *J. Organomet. Chem.* **2013**, *738*, 76−91.
(12) (a) Bose, S.; Ghosh, M.; Ghosh, S. *J. Org. Chem.* **2012**, *77*, 6345−6350. (b) Minger, T. L.; Phillips, A. J. *Tetrahedron Lett.* **2002**, *43*, 5357−5359.
(13) Chauvin, Y.; Herisson, J. *Makromol. Chem.* **1971**, *141*, 161−167.
(14) (a) Becke, A. D. *Phys. Rev. A* **1988**, *38*, 3098−3100. (b) Lee, C.; Yang, W.; Parr, R. G. *Phys. Rev. B* **1988**, *37*, 785−789. (c) Becke, A. D. *J. Chem. Phys.* **1993**, *98*, 5648−5652. (d) Stephens, P. J.; Devlin, F. J.; Chabalowski, C. F.; Frisch, M. J. *J. Phys. Chem.* **1994**, *98*, 11623−11627.
(15) Śliwa, P.; Handzlik, J. *Chem. Phys. Lett.* **2010**, *493*, 273−278.
(16) (a) Liu, P.; Xu, X.; Dong, X.; Keitz, B. K.; Herbert, M. B.; Grubbs, R. H.; Houk, K. N. *J. Am. Chem. Soc.* **2012**, *134*, 1464−1467. (b) Herbert, M. B.; Lan, Y.; Keitz, B. K.; Liu, P.; Endo, K.; Day, M. W.; Houk, K. N.; Grubbs, R. H. *J. Am. Chem. Soc.* **2012**, *134*, 7861−7866. (c) Miyazaki, H.; Herbert, M. B.; Liu, P.; Dong, X.; Xu, X.; Keitz, B. K.; Ung, T.; Mkrtumyan, G.; Houk, K. N.; Grubbs, R. H. *J. Am. Chem. Soc.* **2013**, *135*, 5848−5858.
(17) Marenich, A. V.; Cramer, C. J.; Truhlar, D. G. *J. Phys. Chem. B* **2009**, *113*, 6378−6396.
(18) (a) Vorfalt, T.; Wannowius, K. J.; Plenio, H. *Angew. Chem., Int. Ed.* **2010**, *49*, 5533. (b) Ashworth, I. W.; Hillier, I. H.; Nelson, D. J.; Percy, J. M.; Vincent, M. A. *Chem. Commun.* **2011**, *47*, 5428−5430.
(19) For an explanation of "energy span" and its relation to the kinetics of catalytic cycles, see: Kozuch, S.; Shaik, S. *Acc. Chem. Res.* **2011**, *44*, 101−110.
(20) For a review discussing equilibria in ring-closing metathesis reactions, see: Monfette, S.; Fogg, D. E. *Chem. Rev.* **2009**, *109*, 3783−3816.
(21) See the Supporting Information for details.
(22) For some representative examples of metathesis rearrangements of bicyclo[2.2.2]octene systems, see ref 12.